Measurement of 8-hydroxydeoxyguanosine formation in DNA

Oxidative DNA damage in liver was estimated as the levels of 8-OHdG. 8-OHdG levels in liver DNA were determined using the method described by Umemura et al. (2006). Briefly, nuclear DNA was isolated from 0.3 g of a wet weight sample using a DNA Extractor WB Kit (Wako Pure Chemical Industries) containing an antioxidant NaI solution to dissolve the cellular components. For further prevention of auto-oxidation in the cell-lysis step, deferoxamine mesylate was added to the lysis buffer (Helbock et al. 1998). DNA was digested into deoxynucleotides using nuclease P1 and alkaline phosphatase. The levels of 8-OHdG (8-OHdG/10^5 deoxyguanosine) were then assessed by high-performance liquid chromatography using an electrochemical detection system (Coulochem II; ESA Biosciences, Inc., MA, USA) as previously reported (Umemura et al. 2006).

mRNA expression in whole livers by real-time RT–PCR analysis

In our previous studies (Muguruma et al. 2006, 2007, 2008), PBO upregulated metabolism-related genes involved in oxidative stress and DNA repair-related genes, apoptosis-related genes, and cell cycle-, and cell proliferation-related genes. We also measured genes (oncogene, apoptosis, and cell cycle-regulated genes) that were changed by ROS generation (Vafa et al. 2002; Benhar et al. 2002; Matsumura et al. 2003) (Table 1) using quantitative real-time RT–PCR analysis. Briefly, the total RNA from six mice per treatment group was extracted using TRIzol reagent (Invitrogen, Carlsbad, CA, USA) according to the manufacturer's instructions. The total RNA was reverse transcribed using ThermoScript reverse transcriptase (SuperScript III First-Strand Synthesis System; Invitrogen). All PCRs were performed using Power SYBR Green PCR Master Mix (Applied Biosystems, Foster City, CA, USA) on a Step One Plus (Applied Biosystems) using the following conditions: 1 incubation at 50°C for 2 min followed by 95°C for 10 min, and then 45 incubations at 95°C for 15 s, and 60°C for 1 min. The forward and reverse primers listed in Table 1 were designed using Primer Express 2.0 software following Applied Biosystems' instructions for optimal primer design. The relative differences in gene expression were calculated using the cycle time (Ct) values that were first normalized to β-actin, the endogenous control in the same sample, and then relative to a control Ct value by a 2-$\Delta\Delta$Ct method described in the Applied Biosystems User Bulletin #2 'Relative quantification of gene expression.' The data represent the average fold changes with standard deviation.

Statistical analysis

Statistical analysis was first carried out using the F-test for homogeneity of variance. If the variance was homogeneous, a Student's t-test was applied for comparison, and if it was heterogeneous, the Aspin–Welch's t-test was used. The incidences and multiplicities of proliferative lesions observed in the DEN + PBO and DEN-alone group were analyzed using the $\chi 2$-test.

Results

Body and liver weights and macroscopic examinations

There were no deaths or clinical symptoms related to PBO treatment in any of the groups, but all mice in the DEN + PBO group had liver enlargement at necropsy. The final body weights as well as absolute and relative liver weights are given in Table 2. The absolute and relative liver weights of mice in the DEN + PBO group were significantly higher than those in the DEN-alone group.

Formation of hepatic microsomal ROS in liver DNA

The values of liver microsomal ROS generation in the DEN + PBO and DEN-alone groups were 34.60 ± 18.39 and 89.83 ± 17.45, respectively, and the value in the DEN + PBO group significantly increased when compared with the DEN-alone group (Fig. 1).

Formation of 8-OHdG in liver DNA

HPLC analysis revealed that the 8-OHdG levels in the DEN + PBO and DEN-alone groups were 1.21 ± 0.36 and 1.44 ± 0.26, respectively, and there was no significant difference between these groups (Fig. 1).

Histopathological examination

In HE-stained sections, most liver tissues from the DEN + PBO group contained hepatocellular altered foci, adenomas, or carcinomas, while both groups had a similar incidence of altered hepatocellular foci (Table 3; Fig. 2). There was no difference in the histology of liver proliferative lesions induced between the DEN-alone and DEN + PBO groups. However, the incidence of hepatocellular adenomas in the PBO + DEN and DEN-alone groups was 100 and 40%, respectively. Similarly, the incidence of hepatocellular carcinomas in the PBO + DEN group was significantly higher than that in the DEN-alone group.

Table 1 Sequence of primers used for real-time RT–PCR analysis

Accession no.	Symbol	Description	Forward primer	Reverse primer
NM_009992	*Cyp1a1*	Cytochrome P450, family 1, subfamily a, polypeptide 1	GTGGAGCCTCATGTACCTGGTAAC	TGCCAATCACTGTGTCTAGTTCCT
NM_009997	*Cyp2a5*	Cytochrome P450, family 2, subfamily a, polypeptide 5	ACCAGACAAGTCAGGGGTTG	TTTCCCTCTTCTTTGGCTACC
NM_010000	*Cyp2b9*	Cytochrome P450, family 2, subfamily b, polypeptide 9	CCGGTGTGAGCCGATCA	TGCTCAAGTACCCCCATGTCA
NM_009998	*Cyp2b10*	Cytochrome P450, 2b10, phenobarbital inducible, type b	GCTGTCGTTGAGCCAACCTT	TCTTCCAACGTTCCCCATTG
NM_010902	*Nrf2*	Nuclear factor, erythroid derived 2, like 2	CGACAGAAACCTCCATCTACTGAA	CCTCATCACGTAACATGCTGAAG
NM_008706	*Nqo1*	NAD(P)H dehydrogenase, quinone 1	TGGCCGAACACAAGAAGCT	ATGGCTGGCACCCCAAA
NM_008898	*Por*	P450 (cytochrome) oxidoreductase	GCCTGCCTGAGATCGACAAG	GGGTCGCCTTCTCCGTATGT
NM_010957	*Ogg1*	8-oxoguanine DNA glycosylase 1	GCCAACAAAGAACTGGGAAACT	CAGCATAAGGTCCCCACAGATT
NM_009533	*Xrcc5*	X-ray repair complementing defective repair in Chinese hamster cells 5	AAAGGATGATGAGGCGGCA	CGATGGCGACCATGTTTAACTC
NM_007912	*Egfr*	Epidermal growth factor receptor, transcript variant 2	GAAAGTCTGCCAAGGCACAA	AAGGACCACTTCACAGTTGTT
NM_011697	*Vegfb*	Vascular endothelial growth factor B	AATGCAGATCCTCATGATCCAG	CATTGGCTGTGTTCTTCCAGG
NM_011577	*Tgfb1*	Transforming growth factor, beta 1	GCCTGAGTGGCTGTCTTTTGAC	TGTATTCCGTCTCCTTGGTTCA
NM_010849	*c-Myc*	Myelocytomatosis oncogene	GAGCTGTTTGAAGGCTGGATTT	TCCTGTTGGTGAAGTTCACGTT
NM_010234	*c-Fos*	FBJ osteosarcoma oncogene	GAGGAGGGAGCTGACAGATACACT	AGATTGGCAATCTCAGTCTGCAA
NM_010591	*c-Jun*	Jun oncogene	AAGAACTCGGACCTTCTCAC	GTAGTGGTGATGTGCCCATT
NM_001025093	*Atf2*	Activating transcription factor 2	GACAGTGTCATTGTGGCTGATCA	ACTCATTGAACAAACCCACTTCTTC
NM_007498	*Atf3*	Activating transcription factor 3	CAGCATTTGATATACATGCTCAACCT	TCCGGTGTCCGTCCATTCT
NM_007631	*Ccnd1*	Cyclin D1	CGTGGCCTCTAAGATGAAGGA	TCGGGCCGGATAGAGTTGT
NM_007891	*E2f1*	E2F transcription factor 1	CCAGCGCCTGGCCTATG	GCCTTGATCACTATGACCATCTGTT
NM_009029	*Rb1*	Retinoblastoma 1	GGTCTGCCAACACCCACAA	AGATGTCCCAAATGATTCACCAA
NM_016756	*Cdk2*	Cyclin-dependent kinase 2, transcript variant 2	GCCATTCTCACCGTGTCCTT	GATGGACCCCTCTGCATTGA
NM_009870	*Cdk4*	Cyclin-dependent kinase 4	GGGCCTGCCGGTTGAG	GAAGAAAATCCAGGCCGCTTA
NM_009873	*Cdk6*	Cyclin-dependent kinase 6	GCCCTGAATCACCCGTACTTC	TGGCAGGTGAGAGTTCAGGTT
NM_009877	*P16*	Cyclin-dependent kinase inhibitor 2A (Cdkn2a), transcript variant 1, mRNA	CGCCCCGAACTCTTTCG	CGTGAACGTTGCCCATCA
NM_007669	*P21*	Cyclin-dependent kinase inhibitor 1A (Cdkn1a), transcript variant 1	AAAGTGTGCCGTTGTCTCTT	CGTGACGAAGTAAAGTTCC
NM_009875	*P27*	Cyclin-dependent kinase inhibitor 1B (Cdkn1b), mRNA	AACTAACCCGGGGACTTGGAG	GGCCTGTAGTAGAACTCGG
NM_011640	*p53*	Transformation-related protein 53 (Trp53), transcript variant 1	CGCTGCTCCGATGGTGAT	TCGGGATACAAATTTCCTTCCA
NM_009876	*P57*	Mus musculus cyclin-dependent kinase inhibitor 1C (Cdkn1c)	GCCAATGCGAACGACTTCTT	CGTTCGACGCCTTGTTCTC
NM_007393	*Actb*	Actin, beta, cytoplasmic	AGATTACTGCTCTGGCTCCTAGCA	GCCACCGATCCACAGAGA

Table 2 Changes in body weights, liver weights of male ICR mice given PBO for 25 weeks after DEN initiation

Group	DEN-alone	DEN + PBO
No. of animals	6	15
Final body weight (g)	51.43 ± 6.37	46.38 ± 2.84*
Absolute liver weight (g)	2.91 ± 0.92	8.12 ± 2.52**
Relative liver weight (% body weight)	5.60 ± 1.54	17.42 ± 4.99**

The data represent mean ± SD

*, ** Significantly different from the DEN-alone group at $p < 0.05$ or 0.01 (student's *t*-test)

Table 3 Incidence of liver proliferative lesions in ICR mice given PBO for 25 weeks after DEN initiation

Group	DEN-alone	DEN + PBO
No. of mice examined	8	15
Altered foci and liver tumors		
Incidence (%)		
Altered foci	8 (100)	15 (100)
Adenoma	3 (38)	15 (100)#
Carcinoma	0 (0)	6 (40)#
Multiplicity		
Altered foci	5.85 ± 3.71	4.53 ± 2.06
Adenoma	1.53 ± 2.30	6.26 ± 2.23**
Carcinoma	0 ± 0	0.45 ± 0.67*

The data represent mean ± SD

*, ** Significantly different from the DEN-alone group at $p < 0.05$ or 0.01, respectively (Student's *t*-test or Aspin–Welch's *t*-test)

# $p < 0.05$ versus DEN-alone group (χ^2-test)

Immunohistochemical examinations

Almost all hepatocytes and bile ducts were lightly stained for CK8/18, but hepatocellular altered foci, adenomas, and carcinomas were strongly positive for this antibody. The numbers of CK8/18-positive foci and adenomas were significantly higher in DEN + PBO group than those in the DEN-alone group (Table 4; Fig. 2). The PCNA-positive ratio significantly increased in non-tumor hepatocytes, CK8/18-positive foci, and adenomas in the DEN + PBO group compared with the DEN-alone group.

Differential mRNA expression by real-time RT–PCR analysis

PBO increased the expression of *Cyp1a1*, *Cyp2a5*, *Cyp2b10*, *Por*, NAD(P)H dehydrogenase, quinone 1(*Nqo1*), Myc myelocytomatosis oncogene (*c-Myc*), Cyclin D1 (*Ccnd1*), and E2F transcription factor 1(*E2f1*) but downregulated epidermal growth factor receptor (*Egfr*) and DNA glycosylase 1 (*Ogg1*) (Table 5).

Discussion

PBO increased the incidence of hepatocellular adenomas in CD-1 mice at a dose of 300 mg/kg/day for 79 weeks (Butler et al. 1998). Here, PBO increased the incidence of hepatocellular adenomas and carcinomas, confirming that PBO is a hepatocarcinogen in mice and promotes liver tumor formation. The hepatocellular foci were difficult to identify in HE-stained sections and in frozen sections stained with gamma-glutamyltranspeptidase (GGT). CK18 was overexpressed in hepatocellular carcinomas induced in mice that were exposed transplacentally to arsenic during gestation in mice (Liu et al. 2004). CK8/18 overexpression may drive neoplastic transformation of preneoplastic cells in

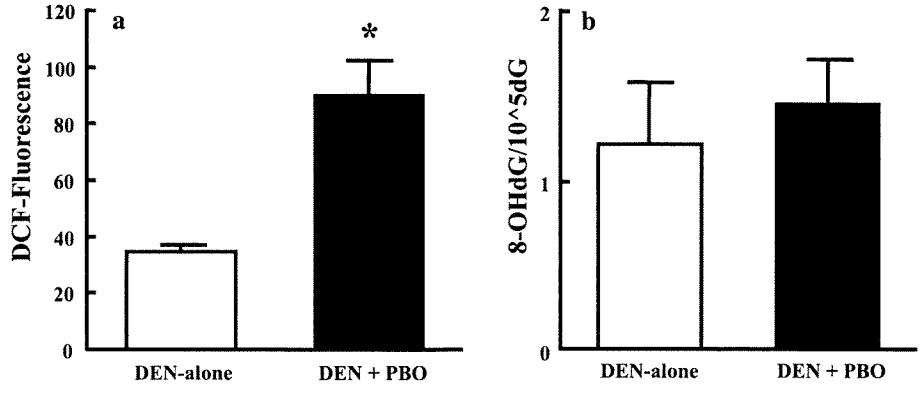

Fig. 1 Oxidative stress markers in mice given PBO for 25 weeks after DEN initiation. **a** NADPH-dependent microsomal ROS production measured by the fluorescent probe, H_2DCFDA. Each column represents the mean + SD of ROS production in isolated liver microsomes from partially hepatectomized mice given DEN-alone (*white column*; $n = 5$) or DEN + PBO (*black column*; $n = 5$). *Significantly different from the DEN-alone group at $p < 0.05$ (Student's *t*-test). **b** 8-OHdG levels in liver DNA. Values are expressed as mean + SD in 5 mice

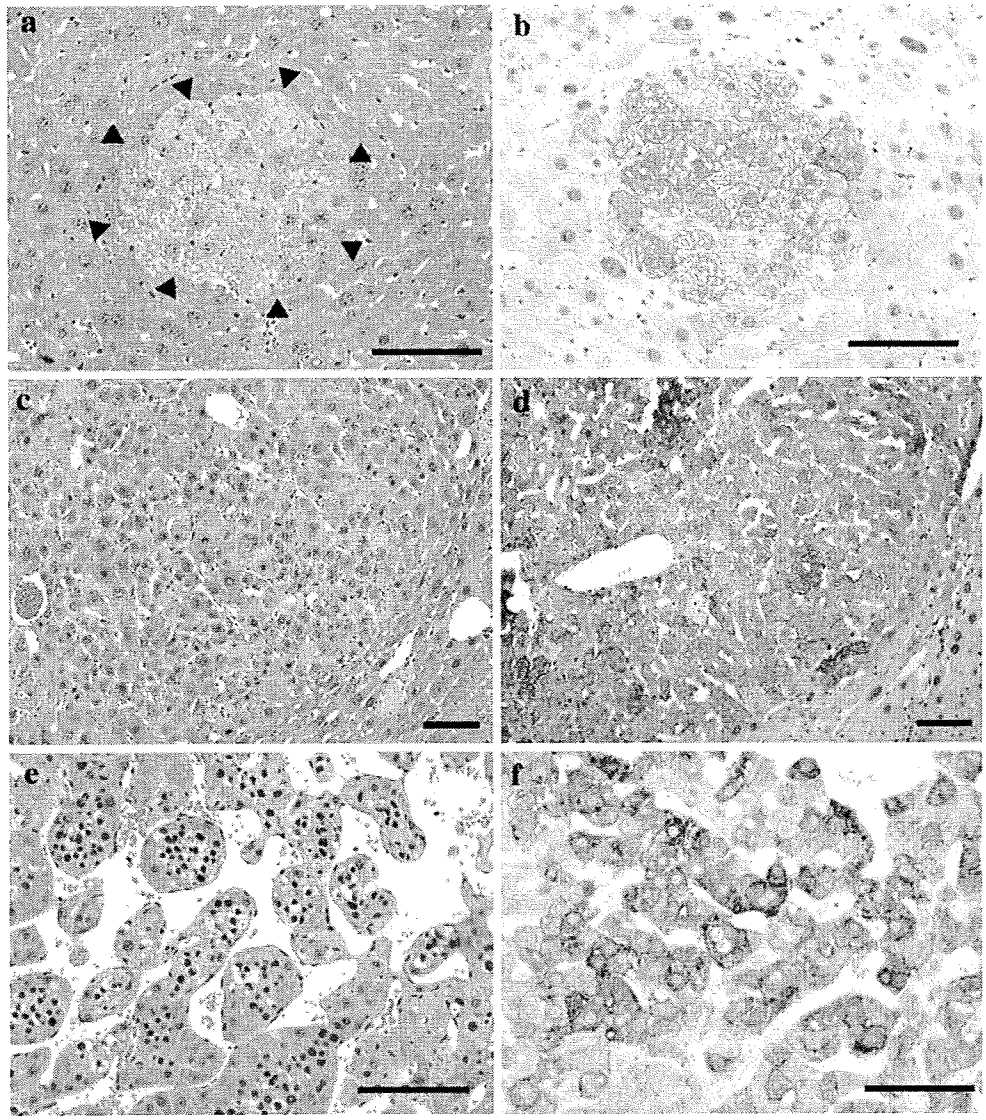

Fig. 2 Light microscopic photographs (**a**, **c**, **d**) and immunohistochemistry of CK8/18 (**c**, **d**, **e**) of hepatocellular proliferative lesions in mice given PBO for 25 weeks after DEN initiation. **a** and **b** altered focus, **c** and **d** adenoma., **e** and **f** carcinoma *Bar* = 100 μm

GST-P-positive foci during rat hepatocarcinogenesis (Kakehashi et al. 2009). We previously reported that the number of CK 8/18-positive altered foci significantly increased in rasH2 mice given fenofibrate for 8 weeks after DEN initiation (Kawai et al. 2008). Here, most of the proliferative lesions were strongly positive for CK8/18 and PBO increased the incidence of CK8/18-positive altered foci, adenomas, and carcinomas. Therefore, the finding obtained suggests that CK8/18 is a specific marker of altered foci, adenomas, and carcinomas in mice.

We previously used microarray analysis and real-time RT–PCR to show increased levels of oxidative and metabolic stress-related genes, *Cyp1a1*, *Cyp2a5*, *Cyp2b9*, *Cyp2b10*, and *Por*, in male ICR mice fed a diet containing 0.6% PBO for 1, 4, and 8 weeks without any initiation treatment (Muguruma et al. 2006). In addition, the expressions of *Ccnd1* (Proliferation-related gene) and *Xrcc5* (DNA damage and repair gene) in PBO-treated mice were significantly higher in tested group than those in the control at each time point and at week 8 only, respectively. PBO also increased NADPH-dependent microsomal ROS production in these mice, although no measurement of 8-OHdG levels was observed in the liver. Since *Xrcc5* is regarded as a DNA repair gene (Difilippantonio et al. 2000), an upregulation of *Xrcc5* appeared to suggest that overt DNA damage might occur in mice treated with PBO for 8 weeks. On the other hand, in the present study, PBO increased the same oxidative and metabolic stress-related genes and *Ccnd1*, but did not increase 8-OHdG or the mRNA expression of *Xrcc5* in mice. De Vizcaya-Ruiz et al. (2008)

Table 4 CK8/18-positive liver lesions and PCNA ratio in male ICR mice given PBO for 25 weeks after DEN initiation

Group	DEN-alone	DEN + PBO
No. of mice examined	8	12
Number of CK 8/18-positive liver lesions (number/cm^2)		
Altered foci	0.46 ± 0.70	2.74 ± 1.78**
Adenomas	0.08 ± 0.22	2.68 ± 1.48**
Carcinomas	0	0.37 ± 0.41
PCNA ratio		
Non-tumor hepatocytes	0.38 ± 0.59	1.44 ± 1.01*
Altered foci	5.39 ± 7.06	23.25 ± 17.06**
Adenomas	6.17 ± 5.45	21.08 ± 14.74**
Carcinomas	0	23.75 ± 14.02

The data represent mean ± SD

*, ** Significantly different from the DEN-alone group at $p < 0.05$, 0.01 (Student's *t*-test or Aspin–Welch's *t*-test)

Table 5 Real-time RT-PCR analysis of livers of male ICR mice given PBO for 25 weeks after DEN initiation

Gene name	DEN-alone	DEN + PBO
No. of animals	5[a]	5
Cyp1a1	1.04 ± 0.33[b]	66.63 ± 39.08**
Cyp2a5	1.06 ± 0.37	8.72 ± 2.76**
Cyp2b9	1.69 ± 1.62	3.83 ± 4.70
Cyp2b10	1.04 ± 0.27	61.46 ± 22.67**
Por	1.01 ± 0.14	4.67 ± 0.65**
Nrf2	1.08 ± 0.46	1.31 ± 0.19
Nqo1	1.01 ± 0.14	4.45 ± 1.10**
Ogg1	1.01 ± 0.19	0.74 ± 0.14*
Xrcc5	1.01 ± 0.17	0.90 ± 0.18
Egfr	1.00 ± 0.11	0.22 ± 0.26**
Vegf	1.03 ± 0.28	0.89 ± 0.33
Tgfb1	1.05 ± 0.34	0.99 ± 0.47
c-Myc	1.17 ± 0.68	2.15 ± 0.45*
c-Fos	1.18 ± 0.60	1.47 ± 0.72
c-Jun	1.09 ± 0.43	1.31 ± 0.99
Atf2	1.08 ± 0.50	0.61 ± 0.09
Atf3	1.50 ± 1.20	2.23 ± 0.94
Ccnd1	1.07 ± 0.42	4.05 ± 1.56**
E2f1	1.01 ± 0.17	1.50 ± 0.39*
Rb1	1.01 ± 0.18	0.95 ± 0.36
Cdk2	1.14 ± 0.64	1.10 ± 0.50
Cdk4	1.03 ± 0.31	0.90 ± 0.26
Cdk6	1.04 ± 0.33	1.29 ± 0.35
P16	1.25 ± 0.85	0.69 ± 0.42
P21	1.14 ± 0.55	0.77 ± 0.38
P27	1.02 ± 0.22	0.80 ± 0.33
P53	1.02 ± 0.24	0.79 ± 0.22
P57	1.01 ± 0.15	1.06 ± 0.39

The data represent mean ± SD

[a] No of animals

[b] Expression level/(β-actin)

*, ** Significantly different from the DEN-alone group at $p < 0.05$ or 0.01, respectively (student's *t*-test or Aspin–Welch's *t*-test)

reported that ROS production leads to DNA damage and upregulation of DNA repair genes. Our previous study in rats demonstrated that PBO generated ROS via metabolic pathways and induced oxidative stress, including oxidative DNA damage, inducing hepatocellular tumors in hepatectomized rats given a diet containing 1 or 2% PBO for 8 weeks after DEN initiation treatment (Muguruma et al. 2007). Therefore, the result of our study may imply that PBO could generate ROS via metabolic pathways, but does not result in DNA damage in mice. The question thus arises as to why 8-OHdG formation occurred in the rat but not in the mouse. In our previous study, the phase II enzyme genes such as *Nqo1*, *UDPGTR-2*, *Gpx2*, *GRx*, and *Slc7a5* that are regulated under the transcriptional factor *Nrf2* were upregulated in hepatectomized rats given PBO for 8 weeks after DEN initiation (Muguruma et al. 2007). Furthermore, the expression level of *Nqo1*, an important part of cellular antioxidant defense by detoxifying quinines which prevents the generation of ROS (Siegel et al. 2004), in PBO-treated rats was three times higher than that in the 0% PBO rats. In addition, the production of ROS and 8-OHdG in the liver of PBO-treated rats also significantly increased in these rats. This signifies that an excess amount of ROS, which could not be eliminated by the upregulation of Nrf-2-mediated phase II enzymes, is produced from the microsomes in PBO-treated rats and results in the formation of 8-OHdG. On the other hand, in our previous another study, in which hepatectomized mice were given a diet containing 0.6% PBO for 8 weeks after DEN initiation, the expression levels of *Cyp1a1*, *Cyp2a5*, *Cyp2b9*, *Cyp2b10*, and *Por* were upregulated in PBO-treated mice. However, only *Nqo1* among the Nrf-2-mediated phase II enzymes was upregulated, and its expression level increased only 1.80-fold (Kawai et al. 2009). In addition, the expression level of *Nrf2* in mice of the DEN + PBO group was 1.7 times higher than the DEN-alone group, and its induction rate is relatively low, when compared with that in the rat study. In the present study, the expression levels of *Nrf2* and *Nqo1* in PBO-treated mice were 1.31 and 4.45, respectively and are not so high. Furthermore, the expression level of *Ogg1*, that is regarded as a 8-OHdG repair enzyme (Kinoshita et al. 2002), significantly decreased in PBO-treated mice. These findings may suggest that the generation of ROS in PBO-treated mice is not so remarkable and will not result in the 8-OHdG formation. However, since we do not have direct evidence explaining the reason why

PBO did not induce oxidative DNA damage irrespective of ROS generation in mice, we must perform further analyses as a future work to clarify the difference in the formation of 8-OHdG between the rat and mouse.

Excessive ROS production and oxidative stress produces a rapid and transient increase in mRNA levels of the early response genes, such as *c-Fos*, *c-Jun*, and *c-Myc* (Iemitsu et al. 2006; Luna et al. 1994; Mattie et al. 2008). Early response genes encode transcription factors and therefore play a role in the regulation of cellular responses following endogenous or exogenous stress (Luna et al. 1994). C-myc induced by ROS generation then regulates the expression of E2F1 (Matsumura et al. 2003; Mann and Jones 1996). E2F1 can suppress NF-kB activity to increase the susceptibility to apoptosis in in vitro transfection studies (Matsumura et al. 2003). c-Myc and E2F1 are higher in lymphoma cells during middle tumor development and, like MAPK, regulate cell proliferation without changing cell size (Panchuk et al. 2008). Sustained overexpression of E2F and c-Myc during the terminal stage of tumor development can increase cell size due to the blockage of G_1/S transition or facilitation of apoptosis. This finding suggests that increased expression of *c-Myc* and *E2f1* during carcinogenesis involves complex phenomena consisting of cell proliferation, cell quiescence, and apoptosis, depending on the stage of tumor development. In addition, the PCNA-positive ratio significantly increased in intact hepatocytes, CK8/18-positive foci, and adenomas in the DEN + PBO group compared with the DEN-alone group. Considering the increased PCNA-positive ratio and *Ccnd1*, and unchanged expression of *p16*, *p21*, *p27*, *p53*, and *p57*, upregulation of *c-Myc* resulting from the excessive ROS production and *E2f1* may reflect for a role on cellular proliferation in hepatocellular proliferative lesions induced by PBO in mice.

Here, PBO decreased *Egfr* levels. EGFR belongs to the family of c-erbB proteins that can heterodimerize for ligand-dependent activation of downstream signaling. Downregulation of EGFR occurs in preneoplastic liver cell foci and neoplastic lesions positive for GST-P after treatment with non-genotoxic hepatocarcinogens early in a rat two-stage hepatocarcinogenesis model (Taniai et al. 2009). We found similar EGFR downregulation in GST-P-positive foci here. EGFR inactivation can be induced through transcriptional silencing by CpG island hypermethylation in tumor cells (Montero et al. 2006) and promote the formation of proliferative lesions in mice and rats. Taking into account the above references, the downregulation of EGFR is considered to play a role for the formation of liver proliferative lesions in mice as well as in rats.

In conclusion, PBO has the potential to generate ROS via the metabolic pathway in the liver of mice but does not induce oxidative DNA damage. Such an excessive ROS production probably activates cell growth involved in c-Myc- and E2F1-related pathways and acts as a liver tumor promoter of DEN-initiated hepatocarcinogenesis in mice.

Acknowledgments This study was partly supported by a grant in-aid for research on the safety of veterinary drug residues in food of animal origin from the Ministry of Health, Labor and Welfare of Japan (H19-shokuhin-ippan-011).

References

Benhar M, Engelberg D, Levitzki A (2002) ROS, stress-activated kinases and stress signaling in cancer. EMBO Rep 3:420–425

Butler WH, Gabriel KL, Osimitz TG, Preiss FJ (1998) Oncogenicity studies of piperonyl butoxide in rats and mice. Hum Exp Toxicol 17:323–330

De Vizcaya-Ruiz A, Barbier O, Ruiz-Ramos R, Cebrian ME (2008) Biomarkers of oxidative stress and damage in human populations exposed to arsenic. Mutat Res 674:85–92

Dewa Y, Nishimura J, Muguruma M, Jin M, Kawai M, Saegusa Y, Okamura T, Umemura T, Mitsumori K (2009) Involvement of oxidative stress in hepatocellular tumor-promoting activity of oxfendazole in rats. Arch Toxicol 83:503–511

Difilippantonio MJ, Zhu J, Chen HT, Meffre E, Nussenzweig MC, Max EE, Ried T, Nussenzweig A (2000) DNA repair protein Ku80 suppresses chromosomal aberrations and malignant transformation. Nature 404:510–514

Helbock HJ, Beckman KB, Shigenaga MK, Walter PB, Woodall AA, Yeo HC, Ames BN (1998) DNA oxidation matters: the HPLC-electrochemical detection assay of 8-oxo-deoxyguanosine and 8-oxo-guanine. Proc Natl Acad Sci USA 95:288–293

Iemitsu M, Maeda S, Jesmin S, Otsuki T, Kasuya Y, Miyauchi T (2006) Activation pattern of MAPK signaling in the hearts of trained and untrained rats following a single bout of exercise. J Appl Physiol 101:151–163

Kakehashi A, Inoue M, Wei M, Fukushima S, Wanibuchi H (2009) Cytokeratin 8/18 overexpression and complex formation as an indicator of GST-P positive foci transformation into hepatocellular carcinomas. Toxicol Appl Pharmacol 238:71–79

Kasai H (1997) Analysis of a form of oxidative DNA damage, 8-hydroxy-2′-deoxyguanosine, as a marker of cellular oxidative stress during carcinogenesis. Mutat Res 387:147–163

Kawai M, Jin M, Nishimura J, Dewa Y, Saegusa Y, Matsumoto S, Taniai E, Shibutani M, Mitsumori K (2008) Hepatocarcinogenic susceptibility of fenofibrate and its possible mechanism of carcinogenicity in a two-stage hepatocarcinogenesis model of rasH2 mice. Toxicol Pathol 36:950–957

Kawai M, Saegusa Y, Jin M, Dewa Y, Nishimura J, Harada T, Shibutani M, Mitsumori K (2009) Mechanistic study on hepatocarcinogenesis of piperonyl butoxide in mice. Toxicol Pathol 37:761–769

Kinoshita A, Wanibuchi H, Imaoka S, Ogawa M, Masuda C, Morimura K, Funae Y, Fukushima S (2002) Formation of 8-hydroxydeoxyguanosine and cell-cycle arrest in the rat liver via generation of oxidative stress by phenobarbital: association with expression profiles of p21(WAF1/Cip1), cyclin D1 and Ogg1. Carcinogenesis 23:341–349

Liu J, Xie Y, Ward JM, Diwan BA, Waalkes MP (2004) Toxicogenomics analysis of aberrant gene expression in liver tumors and non tumorous livers of adult mice exposed in utero to inorganic arsenic. Toxicol Sci 77:249–257

Luna MC, Wong S, Gomer CJ (1994) Photodynamic therapy mediated induction of early response genes. Cancer Res 54:1374–1380

Mann DJ, Jones NC (1996) E2F-1 but not E2F-4 can overcome p16-induced G1 cell-cycle arrest. Curr Biol 6:474–483

Matsumura I, Tanaka H, Kanakura Y (2003) E2F1 and c-Myc in cell growth and death. Cell Cycle 2:333–338

Mattie MD, McElwee MK, Freedman JH (2008) Mechanism of copper-activated transcription: activation of AP-1, and the JNK/SAPK and p38 signal transduction pathways. J Mol Biol 28:1008–1018

Montero AJ, Díaz-Montero CM, Mao L, Youssef EM, Estecio M, Shen L, Issa JP (2006) Epigenetic inactivation of EGFR by CpG island hypermethylation in cancer. Cancer Biol Ther 5:1494–1501

Moto M, Okamura M, Muguruma M, Ito T, Jin M, Kashida Y, Mitsumori K (2006) Gene expression analysis on the dicyclanil-induced hepatocellular tumors mice. Toxicol Pathol 34:744–751

Muguruma M, Nishimura J, Jin M, Kashida Y, Moto M, Takahashi M, Yokouchi Y, Mitsumori K (2006) Molecular pathological analysis for determining the possible mechanism of piperonyl butoxide-induced hepatocarcinogenesis in mice. Toxicology 228:178–187

Muguruma M, Unami A, Kanki M, Kuroiwa Y, Nishimura J, Dewa Y, Umemura T, Oishi Y, Mitsumori K (2007) Possible involvement of oxidative stress in piperonyl butoxide induced hepatocarcinogenesis in rats. Toxicology 236:61–75

Muguruma M, Arai K, Moto M, Nishimura J, Dewa Y, Mitsumori K (2008) Piperonyl butoxide activates c-Jun and ATF-2 in the hepatocytes of mice. Arch Toxicol 82:749–753

Muguruma M, Kawai M, Dewa Y, Nishimura J, Saegusa Y, Yasuno H, Jin M, Matsumoto S, Takabatake M, Arai K, Mitsumori K (2009) Threshold dose of piperonyl butoxide that induces reactive oxygen species-mediated hepatocarcinogenesis in rats. Arch Toxicol 83:83–93

Nishikawa T, Wanibuchi H, Ogawa M, Kinoshita A, Morimura K, Hiroi T, Funae Y, Kishida H, Nakae D, Fukushima S (2002) Promoting effects of monomethylarsonic acid, dimethylarsinic acid and trimethylarsine oxide on induction of rat liver preneoplastic glutathione S-transferase placental form positive foci: a possible reactive oxygen species mechanism. Int J Cancer 100:136–139

Nishimura J, Dewa Y, Muguruma M, Kuroiwa Y, Yasuno H, Shima T, Jin M, Takahashi M, Umemura T, Mitsumori K (2007) Effect of fenofibrate on oxidative DNA damage and on gene expression related to cell proliferation and apoptosis in rats. Toxicol Sci 97:44–54

Okamiya H, Mitsumori K, Onodera H, Ito S, Imazawa T, Yasuhara K, Takahashi M (1998) Mechanistic study on liver tumor promoting effects of piperonyl butoxide in rats. Arch Toxicol 72:744–750

Panchuk RR, Boiko NM, Lootsik MD, Stoika RS (2008) Changes in signaling pathways of cell proliferation and apoptosis during NK/Ly lymphoma aging. Cell Biol Int 32:1057–1063

Puntarulo S, Cederbaum AI (1998) Production of reactive oxygen species by microsomes enriched in specific human cytochrome P450 enzymes. Free Radic Biol Med 24:1324–1330

Siegel D, Gustafson DL, Dehn DL, Han JY, Boonchoong P, Berliner LJ, Ross D (2004) NAD(P)H:quinone oxidoreductase 1: role as a superoxide scavenger. Mol Pharmacol 65:1238–1247

Takahashi O, Oishi S, Fujitani T, Tanaka T, Yoneyama M (1994) Chronic toxicity studies of piperonyl butoxide in F344 rats: induction of hepatocellular carcinoma. Fundament Appl Toxicol 22:293–303

Taniai E, Kawai M, Dewa Y, Nishimura J, Harada T, Saegusa Y, Matsumoto S, Takahashi M, Mitsumori K, Shibutani M (2009) Crosstalk between PTEN/Akt2 and TGFbeta signaling involving EGF receptor downregulation during the tumor promotion process from the early stage in a rat two-stage hepatocarcinogenesis model. Cancer Sci 100:813–820

Umemura T, Kanki K, Kuroiwa Y, Ishii Y, Okano K, Nohmi T, Nishikawa A, Hirose M (2006) In vivo mutagenicity and initiation following oxidative DNA lesion in the kidneys of rats given potassium bromate. Cancer Sci 97:829–835

Vafa O, Wade M, Kern S, Beeche M, Pandita TK, Hampton GM, Wahl GM (2002) c-Myc can induce DNA damage, increase reactive oxygen species, and mitigate p53 function: a mechanism for oncogene-induced genetic instability. Mol Cell 9:1031–1044

Valavanidis A, Vlachogianni T, Fiotakis C (2009) 8-hydroxy-2′-deoxyguanosine (8-OHdG): A critical biomarker of oxidative stress and carcinogenesis. J Environ Sci Health C Environ Carcinog Ecotoxicol 27:120–139

The Journal of Veterinary Medical Science

Cytokeratin 8/18 is a useful immunohistochemical marker for hepatocellular proliferative lesions in mice

Journal:	*The Journal of Veterinary Medical Science*
Manuscript ID:	JVMS-09-0329
Manuscript Type:	Full Paper
Date Submitted by the Author:	29-Jul-2009
Complete List of Authors:	Kawai, Masaomi; Laboratory of Veterinary Pathology, Tokyo University of Agriculture and Technology Saegusa, Yukie; Tokyo University of Agriculture and Technology, Veterinary Medicine kemmochi, Sayaka; Tokyo University of Agriculture and Technology, Veterinary Medicine Harada, Tomoaki; Tokyo University of Agriculture and Technology, Veterinary Medicine Shimamoto, Keisuke; Tokyo University of Agriculture and Technology, Veterinary Medicine Shibutani, Makoto; Tokyo University of Agriculture and Technology, Laboratory of Veterinary Pathology Mitsumori, Kunitoshi; Tokyo University of Agriculture and Technology, Veterinary Medicine
Keywords:	Toxicologic Pathology, Tumor marker, Liver, mouse, immunohistochemistry
Category:	Pathology

Categories: Pathology
Type of Paper: Full paper

Title: Cytokeratin 8/18 is a useful immunohistochemical marker for hepatocellular proliferative lesions in mice

Masaomi Kawawi[1,2], Yukie Saegusa[1,2], Sayaka kemmochi[1,2], Tomoaki Harada[1], Keisuke Shimamoto[1,2], Makoto Shibutani[1] and Kunitoshi Mitsumori[1]

[1]Laboratory of Veterinary Pathology, Tokyo University of Agriculture and Technology, Fuchu-shi, Tokyo 183-8509, Japan

[2]Pathogenetic Veterinary Science, United Graduate School of Veterinary Sciences, Gifu University, Gifu-shi, Gifu 501-1193, Japan

Corresponding Address:

Kunitoshi Mitsumori, D.V.M., Ph.D.

Professor, Laboratory of Veterinary Pathology, Tokyo University of Agriculture and Technology,

3-5-8 Saiwai-cho, Fuchu-shi, Tokyo 183-8509, Japan

Phone & Fax: +81-42-367-5771

Email: mitsumor@cc.tuat.ac.jp

Running head: CK8/18 AS LIVER TUMOR MARKERS IN MICE

Abstract

In order to clarify whether cytokeratin 8/18 (CK8/18) is a useful immunohistochemical marker for hepatocellular proliferative lesions in mice, partially hepatectomized male ICR mice were given 0.6 % piperonyl butoxide (PBO) for 8 (Experiment I) or 27 weeks (Experiment II) after *N*-diethylnitrosamine (DEN)-initiation treatment, and the livers were subjected to histological examinations on hematoxylin-eosin (HE) stained sections, CK8/18 immunohistochemistry and gamma-glutamyl transpeptidase (GGT) histochemistry. In Experiment I, the multiplicity of hepatocellular foci that were observed in HE-stained sections, positive for CK8/18 and positive for GGT was 10.17, 18.50 and 3.50, respectively. In Experiment II, the total multiplicity of hepatocellular foci that were observed in HE-stained sections, positive/negative for CK8/18 and positive/negative for GGT was 4.47, 23.17 and 10.16, respectively. Most of the hepatocellular adenomas and carcinomas observed in HE-stained sections were positive for CK8/18, but some of the adenomas were negative for CK8/18. These findings indicate that more hepatocellular proliferative lesions can be detected in CK8/18 immunohistochemistry in addition to those observed in HE-stained sections, and suggest that CK8/18 may become a useful immunohistochemical marker for detecting hepatocellular proliferative lesions in mice.

Key word: cytokeratin 8/18, liver, mouse, piperonyl butoxide.

INTRODUCTION

The rat liver medium-term bioassay system first established by Ito *et al.* [14] has been repeatedly used for the detection of carcinogenic or tumor promoting potentials of chemical substances and has great advantages due to reproducibility and reliability for generation of data within 8 weeks [8]. For assessment of promoting effects of the test chemicals, glutathione S-transferase placental form (GST-P)-positive cell foci are used as the primary endpoint. Moreover, since production of GST-P foci has been closely correlated with the actual tumor yields [11, 19], they are regarded as reliable preneoplastic lesions in rats. However, it is generally recognized that this immunohistochemical marker is not reactive for liver preneoplastic and neoplastic lesions of mice. It has been shown that gamma-glutamyl transpeptidase (GGT) play a role in multistage hepatocarcinogenesis and the enhanced expression of this enzyme is observed in preneoplastic altered hepatocellular foci, hepatocellular adenomas, and hepatocellular carcinomas in rats and mice [13]. Therefore, GGT is used as a histochemical marker for these proliferative lesions in mice. However, this histochemical staining of GGT is not suitable for routine histopathological examinations, because frozen sections are necessary for this staining. In addition, there is a disadvantage that almost all the proliferative lesions are not always stained with GGT [7]. Therefore, more reliable markers for liver preneoplastic and neoplastic lesions are absolutely necessary in mice.

It has been shown that cytokeratin (CK) 8/18 overexpression may drive neoplastic transformation of preneoplastic cells in GST-P-positive foci during rat hepatocarcinogenesis [16]. Moreover, we previously reported that hepatocellular altered foci induced in rasH2 mice given fenofibrate for 8 weeks after DEN initiation were immunohistochemically stained with CK8/18 [17].

Piperonyl butoxide (PBO) is a pesticide synergist that is widely used with pyrethroids for grain protection and as a domestic insecticide. PBO is a hepatocarcinogen in F344 rats fed a diet containing 1.2% PBO for 2 years ([27]) and CD-1 mice fed a diet containing 300 mg/kg/day PBO for 79 weeks ([4]). In our previous study in which male mice were subjected to a two-thirds partial hepatectomy, followed by N-diethylnitrosamine (DEN) initiation, and given a diet containing 0.6% PBO for eight weeks to clarify the mechanism of PBO-induced hepatocarcinogenesis in mice, the incidence of GGT-positive foci were significantly increased in the DEN + PBO group compared with the DEN-alone group [18].

In the present study, we performed two different experiments using the mouse two-stage hepatocarcinogenesis model subjected to 8- or 27-week tumor promotion treatment of PBO to clarify whether CK8/18 is a useful immunohistochemical marker for hepatocellular altered foci, adenomas, and carcinomas in mice.

MATERIALS AND METHODS

Chemicals

Piperonyl butoxide (PBO), [2-(2-butoxyethoxy)ethoxy]-4,5-methylenedioxy-2-propyltoluene (CAS register number 51-03-6, EU Number piperonyl butoxide, purity 90%), was purchased from Kanto Chemical Co., Inc. (Tokyo, Japan). DEN was purchased from Nacalai Tesque, Inc. (Kyoto, Japan).

Animals and experimental design

Six-week-old male ICR mice were obtained from Japan SLC Inc. (Shizuoka, Japan). They were housed in plastic cages (five animals/cage) with absorbent paper chip bedding in an animal room maintained under standard conditions (room temperature, 22 ± 2 °C; relative humidity, 55% ± 5%; and light/dark cycle, 12 h) and given free access to a powdered diet (Oriental MF; Oriental Yeast, Tokyo, Japan) and tap water. The animals were acclimatized for one week prior to beginning the experiment. The experiment was performed in accordance with the guidelines for animal experimentation of the Tokyo University of Agriculture and Technology.

We performed two different experiments using a short-term two-stage liver carcinogenesis model [21] in mice. In Experiment I, to enhance hepatocellular proliferation, mice were subjected to a two-thirds partial hepatectomy. Twenty-four hours after the

hepatectomy, mice were given a single i.p. injection of DEN (20 mg/kg body weight) dissolved in saline to initiate hepatocarcinogenesis. One week after the DEN injection, 10 animals were given a powdered diet containing 0.6 % PBO for 8 weeks. Nine mice survived in this group, and 6 of 9 mice were subjected to histological examinations including histochemical and immunohistochemical examinations. In Experiment II, mice were similarly subjected to a two-thirds partial hepatectomy. Twelve hour after the hepatectomy, mice were given a single i.p. injection of DEN (20 mg/kg body weight). One week after the injection, 16 animals were given a powdered diet containing 0.6 % PBO for 27 weeks. Fifteen mice survived, and 6 of 15 mice were subjected to the same morphological examinations as the Experiment I.

On completion of treatment, the mice were killed by exsanguination from the posterior vena cava under ether anesthesia, and livers were immersed in 4% paraformaldehyde solution for microscopy. Two sections obtained from different portions of livers/mouse were embedded in OCT compound (Tissue-Tek; Miles Inc., Elkhart, USA) to obtain frozen sections for histochemical evaluation of GGT positive foci, a marker of preneoplastic foci, in mouse livers [7].

Histopathology, histochemical, and immunohistochemical evaluations, and quantitative analyses

After sacrifice, two different sections from the livers fixed in 4% paraformaldehyde were embedded in paraffin, sectioned at 3 μm thickness, and stained with hematoxylin and eosin (HE) for histopathological examinations. The incidence and multiplicity of liver proliferative lesions, such as hepatocellular altered foci, adenomas, and carcinomas, in these HE-stained sections/mouse were counted under a light microscope.

For immunohistochemistry, serial paraffin-embedded liver sections that were continuous to the HE-stained sections were deparaffinized in xylene and rehydrated in ethanol. Anti-cytokeratin 8/18 polyclonal antibody was purchased from PROGEN Biotechnik GmbH (Heidelberg, Germany). The liver sections for CK8/18 were incubated with citrate buffer [0.1 mol/L citrate (pH 6.0)] and heated in a microwave oven at 98 °C for 30 min before incubation with 0.3% hydrogen peroxide in PBS. Non-specific binding sites were blocked with blocking normal serum. The specimens were incubated overnight with the CK8/18 antibody at a dilution of 1:100 in 0.5% casein-PBS at 4 °C. The sections were incubated with a guinea pig peroxidase-conjugated secondary antibody (Fitzgerald Industries International Inc., MA, USA) diluted in PBS supplemented with 0.5% casein. Subsequently, 3, 3'-diaminobenzidine (DAB, Dojindo laboratories, Kumamoto, Japan) was applied as a chromogen. The sections

were finally counterstained with hematoxylin. The incidence and multiplicity of CK8/18-positive and-negative foci, adenomas and carcinomas were counted under a light microscope. The numbers of CK8/18-positive/negative lesions greater than 0.2 mm in diameter were counted.

Histochemical staining of GGT was performed by the modifying methods of Rutenberg *et al.* (1969) [25]. Two frozen sections/mouse obtained from the different portions of livers were cryosectioned and fixed using methanol. After air-drying, a freshly prepared solution containing the substrate, L-glutamic acid-γ-(4-metoxy-β-naphthylamide) (Sigma–Aldrich, St Louis, MO, USA), and fast blue BBN (Wako Pure Chemical Industries, Osaka, Japan) in 0.1 M Tris-buffered saline (pH 7.4) was coated onto the section. Following incubation, the slides were transferred into a 0.1 M cupric sulfate solution. The sections were then stained with hematoxylin and mounted in Apathy's mounting media (Wako Pure Chemical Industries, Osaka, Japan). The incidence and multiplicity of liver proliferative lesions in GGT-stained sections/mouse obtained from two different portions of livers were counted under a light microscope. Single GGT-positive cells were ignored, while the numbers of GGT-positive/negative lesions greater than 0.2 mm in diameter were counted.

RESULTS

Experiment I

In HE-stained sections, all treated mice had hepatocellular altered foci (Table 1). In immunohistochemistry, CK8/18-positive foci were observed in all treated mice. In these mice, hepatocellular foci observed in HE-stained sections were positive for CK8/18 (Figs. 1a-c), but foci that could not be detected in HE-stained sections were also positive for CK8/18. GGT histochemistry revealed that all treated mice had GGT-positive foci, but the number of GGT-positive foci was lower than that of hepatocellular foci observed in HE-stained sections. The multiplicity of hepatocellular foci from the treated mice that were observed in HE-stained sections, positive for CK8/18 and positive for GGT was 10.17, 18.5 and 3.50, respectively.

Neither hepatocellular adenomas nor carcinomas were observed in these treated mice.

Experiment II

Hepatocellular foci: In HE-stained sections, all treated mice had hepatocellular altered foci (Table 2). These foci are composed of eosinophilic, basophilic or clear cell type. In immunohistochemistry, CK8/18-positive foci were observed in all treated mice. In these mice, hepatocellular foci observed in HE-stained sections were positive for CK8/18, but foci that could not be detected in HE-stained sections were also positive for CK8/18. These CK8/18-positive foci were mainly composed of eosinophilic cell type. In addition, hepatocellular foci that are negative for CK8/18 were observed in 5 of 6 mice (83 %). These

CK8/18-negative foci were composed of basophilic or clear cell type. GGT histochemistry revealed that all treated mice had GGT-positive foci, but GGT-negative foci were noted in 2 of 6 mice (17 %). The multiplicity of hepatocellular foci from the treated mice that were observed in HE-stained sections, positive for CK8/18 and positive for GGT was 4.47, 19.67 and 9.83, respectively. In addition, the multiplicity of hepatocellular foci negative for CK8/18 and GGT was 3.50 and 0.33, respectively. The total multiplicity of hepatocellular foci from the treated mice that were observed in HE-stained sections, positive/negative for CK8/18 and positive/negative for GGT was 4.47, 23.17 and 10.16, respectively.

Hepatocellular adenomas: In HE-stained sections, all treated mice had hepatocellular adenomas (Table 2). In immunohistochemistry, CK8/18-positive adenomas were observed in all treated mice. In these mice, hepatocellular adenomas observed in HE-stained sections were positive for CK8/18 (Figs. 1d-e). These CK8/18-positive adenomas were mainly composed of eosinophilic cell type. In addition, hepatocellular adenomas that are negative for CK8/18 were observed in 4 of 6 mice (67 %). These CK8/18-negative adenomas were composed of basophilic or clear cell type (Figs. 1j-m). GGT histochemistry revealed that 5 of 6 treated mice (83 %) had GGT-positive adenomas, but GGT-negative adenomas were also noted in 5 of 6 mice (83 %). The multiplicity of hepatocellular adenomas from the treated mice that were observed in HE-stained sections, positive for CK8/18 and positive for GGT was 11.17, 9.83

and 2.83, respectively. In addition, the multiplicity of hepatocellular adenomas negative for CK8/18 and GGT was 1.33 and 2.67, respectively. The total multiplicity of hepatocellular adenomas from the treated mice that were observed in HE-stained sections, positive/negative for CK8/18 and positive/negative for GGT was 11.17, 11.17 and 5.50, respectively.

Hepatocellular carcinomas: In HE-stained sections, 3 of 6 treated mice (50 %) had hepatocellular carcinomas (Table 2). In immunohistochemistry, these carcinomas were also positive for CK8/18 (Figs. 1g-h). There were no hepatocellular carcinomas that were negative for CK8/18 in these treated mice. GGT histochemistry revealed that 1 of 6 treated mice (17 %) had GGT-positive carcinomas (Fig. 1i), but GGT-negative carcinomas were also noted in 2 of 6 mice (33 %). The multiplicity of hepatocellular carcinomas from the treated mice that were observed in HE-stained sections, positive for CK8/18 and positive for GGT was 1.50, 1.50 and 0.17, respectively. In addition, the multiplicity of hepatocellular carcinomas negative for CK8/18 and GGT was 0 and 0.29, respectively. The total multiplicity of hepatocellular carcinomas from the treated mice that were observed in HE-stained sections, positive for CK8/18 and positive/negative for GGT was 1.50, 1.50 and 0.50, respectively.